



7-26-2012

# Tail Assisted Dynamic Self Righting

Aaron M. Johnson  
*University of Pennsylvania*

Thomas Libby  
*University of California, Berkeley*

Evan Chang-Siu  
*University of California, Berkeley*

Masayoshi Tomizuka  
*University of California, Berkeley*

Robert J. Full  
*University of California, Berkeley*

*See next page for additional authors*

---

BibTeX entry

```
@inproceedings{paper:johnson_clawar_2012, Author = {Aaron M. Johnson and Thomas Libby and Evan Chang-Siu and Masayoshi Tomizuka and Robert J. Full and D. E. Koditschek}, booktitle={Proceedings of the Fifteenth International Conference on Climbing and Walking Robots}, title = {Tail Assisted Dynamic Self Righting}, month = {July}, year = {2012}, pages = {611-620} }
```

This paper is posted at Scholarly Commons. [http://repository.upenn.edu/ese\\_papers/650](http://repository.upenn.edu/ese_papers/650)  
For more information, please contact [repository@pobox.upenn.edu](mailto:repository@pobox.upenn.edu).

---

# Tail Assisted Dynamic Self Righting

## Abstract

In this paper we explore the design space of tails intended for self-righting a robot's body during free fall. Conservation of total angular momentum imposes a dimensionless index of rotational efficacy upon the robot's kinematic and dynamical parameters whose selection insures that for a given tail rotation, the body rotation will be identical at any size scale. In contrast, the duration of such a body reorientation depends upon the acceleration of the tail relative to the body, and power density of the tail's actuator must increase with size in order to achieve the same maneuver in the same relative time. Assuming a simple controller and power-limited actuator, we consider maneuverability constraints upon two different types of parameters — morphological and energetic — that can be used for design. We show how these constraints inform contrasting tail design on two robots separated by a four-fold length scale, the 177g Tailbot and the 8.1kg X-RHex Lite (XRL). We compare previously published empirical self-righting behavior of the Tailbot with new, tailed XRL experiments wherein we drop it nose first from a 2.7 body length height and also deliberately run it off an elevated cliff to land safely on its springy legs in both cases.

This was supported primarily by the ARL/GDRS RCTA and the NSF CiBER-IGERT under Award DGE-0903711.

For more information: [Kod\\*Lab](#)

## Comments

BibTeX entry

```
@inproceedings{paper:johnson_clawar_2012, Author = {Aaron M. Johnson and Thomas Libby and Evan Chang-Siu and Masayoshi Tomizuka and Robert J. Full and D. E. Koditschek}, booktitle={Proceedings of the Fifteenth International Conference on Climbing and Walking Robots}, title = {Tail Assisted Dynamic Self Righting}, month = {July}, year = {2012}, pages = {611--620} }
```

## Author(s)

Aaron M. Johnson, Thomas Libby, Evan Chang-Siu, Masayoshi Tomizuka, Robert J. Full, and Daniel E. Koditschek

## Tail Assisted Dynamic Self Righting

Aaron M. Johnson\*, Thomas Libby†, Evan Chang-Siu†

Masayoshi Tomizuka†, Robert J. Full†, and D. E. Koditschek\*

\* *University of Pennsylvania, 200 S. 33rd St, Philadelphia, PA 19104*

*E-mail: {aaronjoh,kod}@seas.upenn.edu*

† *University of California Berkeley, 1099 Valley Life Science Bldg, Berkeley, CA 94720*

*E-mail: {tlibby,evancs,tomizuka,rjfull}@berkeley.edu*

In this paper we explore the design space of tails intended for self-righting a robot's body during free fall. Conservation of total angular momentum imposes a dimensionless index of rotational efficacy upon the robot's kinematic and dynamical parameters whose selection insures that for a given tail rotation, the body rotation will be identical at any size scale. In contrast, the duration of such a body reorientation depends upon the acceleration of the tail relative to the body, and power density of the tail's actuator must increase with size in order to achieve the same maneuver in the same relative time. Assuming a simple controller and power-limited actuator, we consider maneuverability constraints upon two different types of parameters — morphological and energetic — that can be used for design. We show how these constraints inform contrasting tail design on two robots separated by a four-fold length scale, the 177g Tailbot and the 8.1kg X-RHex Lite (XRL). We compare previously published empirical self-righting behavior of the Tailbot with new, tailed XRL experiments wherein we drop it nose first from a 2.7 body length height and also deliberately run it off an elevated cliff to land safely on its springy legs in both cases.

*Keywords:* Tails, Angular Momentum, Motor Selection, Legged Robots

### 1. Introduction

Tails play a variety of roles in animals, from fat storage<sup>1</sup> to communication.<sup>2</sup> Perhaps more useful to mobile robotics is their ability to stabilize dynamic locomotion. By swinging their tails, geckos can self-right in less than a body length after a fall, or reorient through zero net angular momentum maneuvers.<sup>3</sup> Fast-running lizards use their tails to briefly store angular momentum after a perturbation, enabling feedback-driven attitude control during short leaps.<sup>4</sup> The effectiveness of this mechanism inspired Tailbot (Figure 1(a)), a robot with an active tail which enabled disturbance regulation<sup>4</sup> and other dynamic behaviors, including air-righting and traversing

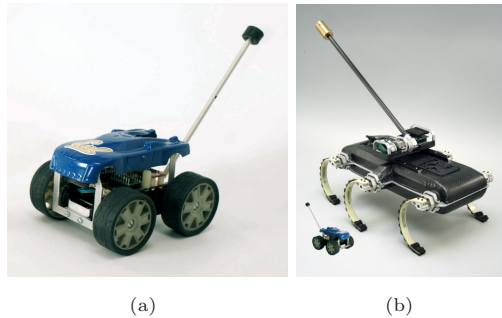


Fig. 1. (a) Tailbot<sup>4, 5</sup> (b) XRL<sup>7, 8</sup> with a new tail, and with approximately sized image of Tailbot inserted.

rough terrain.<sup>5</sup> The stabilizing function of tails appears to operate effectively over a wide range of size scales in natural systems, from 1g geckos to 10 kg lemurs,<sup>6</sup> and possibly beyond. In this paper we explore the efficacy of a stabilizing tail on robots across a range of size scales and provide insight into the design choices. As a second robotic example, we design a tail for X-RHex Lite (XRL)<sup>7, 8</sup> (Figure 1(b)), a relative of the RHex hexapedal robot,<sup>9</sup> over 60 times more massive than Tailbot.

While tails can provide many benefits to mobile robots, here we focus exclusively on aerial self-righting. In general, if survivability or required performance is very sensitive to orientation, an inertial tail will be beneficial, and we treat on the problem of determining criteria for and then assessing empirically the capabilities of a “good” inertial tail. Designing a robot with a tail, or adding one to an existing design, has many costs, including the extra mass, volume and extended body envelope as well as the added complexity and new opportunities for failure. Weighing the penalties associated with these multi-faceted disadvantages against the benefits of increased maneuverability lies far beyond the scope of this paper whose contribution is to address the much narrower question of how to parametrize the design space and then how to select within it a design for a self-righting tail.

In general, we would consider a tail-like design to be one which adds an appendage to a robot, specialized for inertial manipulation (as opposed to say a flywheel<sup>5</sup>). Even then, potential designs can still be quite varied in attachment and mass distribution. Given that the robots in question are intended to navigate through unstructured environments, a tail that trails behind the body and presents few opportunities for entanglement seems preferable to more exotic alternatives. In this case, concentrating mass at

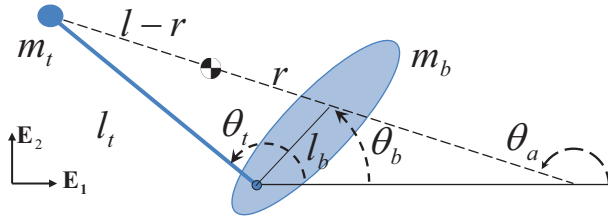


Fig. 2. Planar two body model.

the tail's tip generates the largest moment of inertia per unit mass. In this paper we will consider a point-mass tail at the end of a massless rod; the derivation provided is easily adaptable to other situations by adding the tail's moment of inertia about its center of mass.

The paper's organization roughly parallels the sequence of design and assessment steps associated with the natural stages of tail development. Section 2 proposes a morphological design space (the tail's kinematic and dynamic parameters) and imposes upon it a scale-independent measure of kinematic efficacy arising from conservation of angular momentum. Section 3 introduces the maneuverability task space (the elapsed time and body angle parameters) along with a power train design space (the tail actuator's motor and gearing parameters) and uses the trajectories resulting from a simple (linear) dynamical system model to bind these three parameter spaces together in a constraint that affords the expression of contrasting design criteria<sup>a</sup>. Section 5 presents the empirical results on XRL.

## 2. Kinematics

Consider a simple planar model of a tailed robot in an aerial maneuver, representing the tail by a point mass held by a massless rigid rod, and the rest of the vehicle represented by a single rigid body (Figure 2). The body and tail centers of mass are separated by a length  $l$  with angle  $\theta_a$ , which is dependent on the joint angle  $\theta_r = \theta_b - \theta_t$ . Without loss of generality we assume that the origin is at the COM of the system and therefore the constant total angular momentum,  $H_0$ , about the system's center of mass,<sup>4</sup>

$$H_0 = I_a \dot{\theta}_a + I_b \dot{\theta}_b; \quad I_a = \frac{m_b m_t}{m_b + m_t} l_t^2, \quad (1)$$

<sup>a</sup>We contrast with this simplified linear design model the kinematics (and some behavioral implications) of the general nonlinear case, but for the sake of space leave the detailed derivations in this and other sections to a technical report [12].

imposes a non-holonomic constraint on the dynamics (see the technical report<sup>10</sup> for full derivation)<sup>b</sup>. If the tail pivots at the body center of mass ( $l_b = 0$ ), then  $\dot{\theta}_a = \dot{\theta}_t$  and  $l = l_t = \text{const.}$ , and the constraint is linear in segment angular rates. We choose a time scale  $\gamma$  (units of  $1/s$ , see further discussion in the next section) such that  $t^* = \gamma t$ , where the  $*$  indicates dimensionless values. Substituting the dimensionless derivatives  $\dot{\theta}_i = \gamma \dot{\theta}_i^*$ , simplifying and dividing by  $I_b$  yields a dimensionless version of Eqn. (1),

$$\bar{H}_0 = \varepsilon \dot{\theta}_t^* + \dot{\theta}_b^*; \quad \varepsilon = \frac{I_a}{I_b}; \quad (2)$$

where we define  $\varepsilon$  to be tail *effectiveness* (generalizing the previous definition<sup>4</sup>) and  $\bar{H}_0 = H_0/(\gamma I_b)$  is a dimensionless momentum.

The effectiveness directly governs performance in two distinct tasks: zero angular momentum righting ( $\bar{H}_0 = 0$ ), where  $\varepsilon$  is the ratio of segment speeds, and orientation regulation after an impulse, where a controller tries to maintain a stable body angle ( $\dot{\theta}_b^* = 0$ ) with a tail velocity ( $\dot{\theta}_t^* = \bar{H}_0/\varepsilon$ ). Because effectiveness is dimensionless, isometrically<sup>11</sup> scaled robots are kinematically similar — for a given tail rotation, the body rotation will be identical at any size scale. It is important to note that motor and gearbox selection have no impact on the effectiveness,  $\varepsilon$ , though they will impact righting duration and power requirements, hence this notion of effectiveness decouples the mechanics of tail design from the energetics of motor and gearbox selection.

When the tail pivot is not at the center of mass of the body ( $l_b \neq 0$ ), the kinematics change with  $\theta_r$ , leading to the nonlinear version of (1),<sup>10</sup>

$$\bar{H}_0 = \varepsilon(1 - \lambda \cos \theta_r) \dot{\theta}_t^* + (\varepsilon(\lambda^2 - \lambda \cos \theta_r) + 1) \dot{\theta}_b^*; \quad \lambda = l_b/l_t. \quad (3)$$

This equation governs both stabilization and zero angular momentum maneuvering. In the latter case,  $\bar{H}_0 = 0$ , and by maintaining our definition of effectiveness in righting as the ratio of segment speeds, the configuration-dependent *non-linear effectiveness* is,

$$\varepsilon_n = -\frac{\dot{\theta}_b^*}{\dot{\theta}_t^*} = \frac{\varepsilon(1 - \lambda \cos(\theta_r))}{\varepsilon(\lambda^2 - \lambda \cos(\theta_r)) + 1}. \quad (4)$$

Because we have limited our dynamical analysis, below, to the (linear) case  $\lambda = 0$ , and only report XRL experiments for a tail mounted as close to this condition as could be readily implemented we merely suggest in the

<sup>b</sup> $I_a$  is conventionally called the *reduced mass* moment of inertia. To consider a non-point mass tail, another term  $I_t \dot{\theta}_t$  must be added to  $H_0$ .

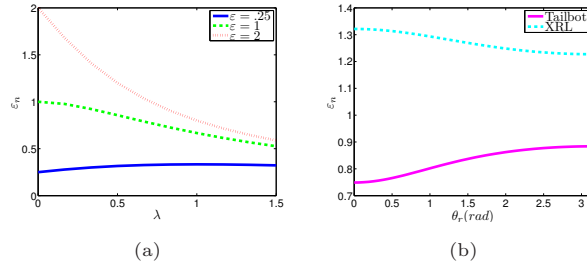


Fig. 3. Variation of non-linear effectiveness with changing  $\lambda$  when  $\theta_r = \pi$  (a), and with respect to  $\theta_r$  for the two robots (b).

numerical plots of Figure 3(a) the somewhat unintuitive manner in which  $\varepsilon_n$  varies in  $\lambda$  and  $\theta_r$ . The effect of joint offset is relatively small — for  $\varepsilon = 1$ ,  $\lambda = 0.5$ ,  $\varepsilon_n$  decreases by only 15-33% depending on tail angle. For robots like Tailbot and XRL with with  $\varepsilon \approx 1$  ( $\varepsilon_{Tailbot} = 1, \varepsilon_{XRL} = 1.29$ ) and  $\lambda < 0.5$  ( $\lambda_{Tailbot} = 0.43, \lambda_{XRL} = 0.14$ ), the change in effectiveness with  $\theta_r$  is small ( $< 25\%$ ) further motivating the linear approximation.

### 3. Dynamics and Power Scaling for a Free Fall Task

While all isometrically scaled robots will maneuver with similar kinematics given enough time, a real terrestrial robot is constrained by the duration of its aerial phase (fall, leap, or other dynamic behavior) and this imposes a new set of requirements on a new set of parameters that specify the tail actuation power train.

Consider a maneuverability task specified by the requirement to reorient the body through a fixed angle  $\theta_b = \theta_0$ , in a desired time  $t = t_0$ . We develop in the technical report<sup>10</sup> the linear (assuming  $\lambda = 0$ ) dynamics associated with a bang-bang style of control (i.e., accelerating and then decelerating the tail with maximal available torque) imparted by a conventionally power-limited actuator (i.e., whose maximal available torque must decrease linearly with speed.<sup>12</sup> Here we restrict our task to a simple reorientation maneuver through a fixed angle  $\theta_b = \theta_0$ , in a desired time  $t = t_0$ . The closed form trajectory of the body angle is,<sup>10</sup>

$$\theta_b(t^*) = \frac{\omega_m}{\gamma(1 + \frac{1}{\varepsilon})} (-1 + t^* + \exp(-t^*)) \quad (5)$$

where the dimensionless state variables are denoted with a \*, for some time scale  $t^* = \gamma t$ , with  $\gamma = \frac{4P(1+1/\varepsilon)}{I_b \omega_m^2}$ ,  $\omega_m$  the motor no-load speed (after the gear box), and  $P$  the motor's peak rated mechanical power.

Thus for a fixed system and time,  $t^* = \gamma t_0$ , we see that the robot body has rotated  $\theta_b(\gamma t_0)$ . Conversely if we desire a body rotation of  $\theta_0$ , we must solve the implicit function  $t^*(\theta_0)/\gamma$  to find the time required.

We can also turn this problem around and ask for a given task specification, a  $\theta_0$  body rotation in  $t_0$ , what are the constraints on the system parameters? If the gearing,  $\omega_m$ , is chosen to minimize the power,  $P$ , then,<sup>10</sup>

$$\theta_0 = \frac{2t_0^{3/2} P^{1/2} k_1}{(1 + 1/\varepsilon)^{1/2} I_b^{1/2}} \quad (6)$$

for constant  $k_1 \approx 0.402$ . Therefore the minimum power required is,

$$P = \frac{\theta_0^2}{4t_0^3 k_1^2} (1 + 1/\varepsilon) I_b \quad (7)$$

but of wider interest may be power density,  $P_d = P/m$ .

This relationship reveals an important constraint on dynamic tail reorientation: the effect of robot size. Consider a robot isometrically scaled by a length scale  $L$ . Then mass  $m$  we will scale by the cube of length  $L$  and  $I_b \propto L^5$ . If the robot were required to reorient through the same angle in the same time regardless of size, then by substitution into Eq. (7) we would require power density  $P_d \propto L^2$ . However, a larger robot will fall slower relative to its length. Considering a free falling distance  $h \propto L$  implies that the time available  $t \propto L^{1/2}$ . Therefore, from Eq. (7) the power density,

$$P_d \propto \frac{1}{L^3} \frac{1}{L^{3/2}} L^5 = L^{1/2} \quad (8)$$

scales as the square root of length. This indicates that inertial reorientation gets more expensive at large size scales; larger robots may suffer reduced performance, or must dedicate a growing portion of total body mass to tail actuation. However, the robots in this paper span a characteristic length range of almost four fold without dramatic differences in ability; in this case, variance in motor power density may trump scaling.

#### 4. XRL Tail Design

In accord with the scale independent features of the mechanical design space introduced in Section 2, the XRL tail is an appropriately scaled approximation to that of Tailbot,<sup>5</sup> both comprising an approximate point-mass made of brass at about 1/10th body mass, attached to a carbon fiber tube of about one body length (see Table 1 for exact values). While Tailbot was a special-built machine, the tail for XRL must be added to an existing platform as a modular payload,<sup>8</sup> and as such the range of motion is



Attribute	Tailbot	XRL + Tail
Body Dimensions (cm)	12x9.3x7.0	51x40x10
Body Mass (kg)	0.16	8.1
Tail Mass (kg)	0.017	0.6
Body Inertia (kgm <sup>2</sup> )	1.54x10 <sup>-4</sup>	0.15
Tail Range of Motion	225°	155°
Linear Effectiveness, $\varepsilon$	1	1.29
Tail Offset, $\lambda$	0.43	0.14
Peak Motor Power (W)	27	342

Table 1. Comparison of Physical Properties.

significantly lower than Tailbot's, especially given a 7.5° safety margin to avoid collision with the body. To compensate, the XRL tail design targets a slightly higher effectiveness so as to afford the same 90° body correction capability as Tailbot.

To mitigate the integration task, both Tailbot's and XRLs tail actuators are chosen to be the same as their wheel/leg motors. But to maximize the performance of the tail, a more careful study is needed. As a slight variation from the previous section, here the power is given for each motor and we now seek to determine the minimal completion time as a function of peak power (parametrized by morphology) rather than the inverse function as above. The time requirement  $t_0$  from the previous section can be thought of a constraint, while here for those motors that meet that constraint we want to consider the fastest completion time as a metric. The optimal no load speed (after gear ratio) and resulting completion time functions are (see the technical report<sup>10</sup> for full derivation),

$$\omega_m = \left( \frac{\theta_0 \beta_0}{k_1 k_0^{3/2}} \right)^{1/3} ; \quad t = \left( \frac{\theta_0^2}{4P k_1^2} (1 + 1/\varepsilon) I_b \right)^{1/3} \quad (9)$$

Other metrics to consider are physical (size, mass), electrical (current and voltage available), and thermal. The thermal cost of a tail for inertial self-righting is in general small due to the very small time scales, however some motors may still overheat. Now, following,<sup>13</sup> whose numerical optimization step does not require the restriction to the linear dynamics ( $\lambda = 0$ ) used to derive (9) and which can incorporate these additional metrics, the performance of all commercial motors<sup>14</sup> can be compared, or used as a constraint

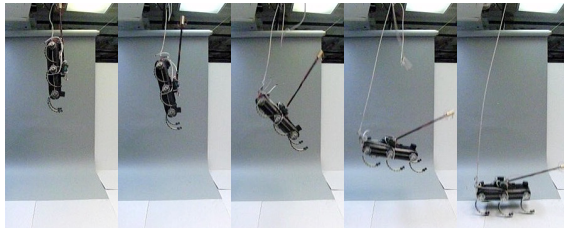


Fig. 4. XRL self-righting in a fall.

in the gearbox optimization. Out of the 1,546 motors considered, 82 of them met the length ( $< 30\text{mm}$ ), weight ( $< 200\text{g}$ ), and minimum completion time ( $< 0.5\text{s}$ ) requirements. Of those, the chosen motor was the third fastest, only 22% slower than what would be the optimal motor. The optimal gear ratio for our motor would be 27:1, the 28:1 gear ratio used is the closest commercially available<sup>c</sup>.

## 5. Experiments

As an empirical validation of the foregoing scaling arguments, we conducted a series of initial tests (Figure 4) to see how large a body rotation can be achieved by a relative tail rotation of about  $155^\circ$ , which is limited by geometry. The robot was dropped nose first from a height of 1.36m (over 8 times the standing height and 2.7 times the body length). The body angle was measured from an IMU and regulated to horizontal by a simple PD controller. This test used the entire  $155^\circ$  range of relative tail motion, rotating the body a maximum of  $89.7^\circ$  before hitting the hard stop. From these two final positions we can calculate an average  $\varepsilon_n = 1.38$ , which matches our simulated result in Fig 3(b) to within 7% and is reasonable considering the errors involved in measuring inertia<sup>15</sup> and manufacturing. As a comparison, the robot was also dropped with no tail activation, causing the front two legs to snap as well as some minor internal damage. Thus if the robot tasks requires a fall from this height, it is definitely survivable assuming it successfully reorients to land within about  $5^\circ$  of level<sup>d</sup>.

To demonstrate this new ability for XRL in a practical task, the second set of experiments was conducted outdoors, running along and then away from a 62 cm (3.8 times the hip height or 1.2 body-length) cliff. The robot's

<sup>c</sup>This analysis could be made more accurate by considering a current limit and more complicated controller.

<sup>d</sup>This is an empirical bound still subject to further tests.



Fig. 5. XRL surviving a run off a cliff outdoors.

inertial sensors detect the cliff upon initial body pitch, then actuate the tail according to the previously described closed loop control policy, and the robot lands on its feet (Figure 5). Another test with XRL running from a cliff with a *passive* tail confirmed that it would land nose first.

## 6. Conclusion

Robots at a range of sizes could benefit from a tail for inertial self-righting. Here we have shown that the kinematics will scale isometrically and are decoupled from the motor/gearbox selection. We have addressed the power considerations for different size robots, but also demonstrated the performance of tails on two robots with vastly different masses and morphologies. In the future we will explore other tail based behaviors.

A fascinating question that also lies largely beyond the scope of this paper surrounds the relative efficacy of appendage (here, a tail) vs. core (body trunk, as in Mather et al.<sup>16</sup>) actuation for the self-righting task. The primary advantages relative to the addition of a tail are that back bending preserves the overall morphology (diminishing the expansion of volume and body envelope) and essentially separates the body into two chunks with much lower moment of inertia, while a tail extends the body envelope and should see a larger effective inertia, depending upon where it is mounted with respect to the body's mass center. However, the penalty in bending is that the final orientation of both segments is important if the legs of the robot are to hit the ground simultaneously.<sup>16</sup> Further, the benefit of a more compact overall body envelope in a new design actually represents a significant deterrent for improving existing robotic platforms like RHex, whose core body structure cannot be substantially altered (without a major redesign<sup>8</sup>) but whose distal appendages can be relatively easily changed, added, or subtracted. We have shown that a tail can enable rapid rotations of up to  $90^\circ$  with relatively low added mass (10% – 20% of body mass), and that the effect of offsetting the tail joint can be relatively low<sup>e</sup>.

<sup>e</sup>Although this preliminary design study simplifies the dynamics and diminishes the

## Acknowledgments

This was supported primarily by the ARL/GDRS RCTA and the NSF CiBER-IGERT under Award DGE-0903711. The authors would like to thank Praveer Nidamaluri for building the X-RHex tail, as well as David Hallac, Justin Starr, Avik De, Ryan Knopf, Mike Choi, Joseph Coto, and Adam Farabaugh for help with the robot and experiments.

## References

1. M. Aleksiuik, *Journal of Mammalogy* **51**, pp. 145 (1970).
2. E. Palagi, *Journal of Comparative Psychology* **123**, p. 1 (2009).
3. A. Jusufi, D. T. Kawano, T. Libby and R. J. Full, *Bioinspiration & Biomimetics* **5**, p. 045001 (2010).
4. T. Libby, T. Y. Moore, E. Chang-Siu, D. Li, D. J. Cohen, A. Jusufi and R. J. Full, *Nature* **481**, 181 (2012).
5. E. Chang-Siu, T. Libby, M. Tomizuka and R. J. Full, A lizard-inspired active tail enables rapid maneuvers and dynamic stabilization in a terrestrial robot, in *Intelligent Robots and Systems*, (San Francisco, CA, USA, 2011).
6. D. C. Dunbar, *American Journal of Primatology* **16**, 291 (1988).
7. K. C. Galloway, G. C. Haynes, B. D. Ilhan, A. M. Johnson, R. Knopf, G. Lynch, B. Plotnick, M. White and D. E. Koditschek, *X-RHex: A Highly Mobile Hexapedal Robot for Sensorimotor Tasks*, tech. rep., University of Pennsylvania (2010).
8. G. C. Haynes, J. Pusey, R. Knopf, A. M. Johnson and D. E. Koditschek, *Laboratory on Legs: An Architecture for Adjustable Morphology with Legged Robots*, in *SPIE Unmanned Systems Technology XIV (8387)*, 2012, p. (in press).
9. U. Saranli, M. Buehler and D. E. Koditschek, *The International Journal of Robotics Research* **20**, 616 (2001).
10. A. M. Johnson, T. Libby, E. Chang-Siu, M. Tomizuka, R. J. Full and D. E. Koditschek, *Tail Assisted Dynamic Self Righting: Full Derivations*, tech. rep., University of Pennsylvania (2012).
11. T. Blackburn and K. Gaston, *Trends in Ecology & Evolution* **9**, 471 (1994).
12. P. Gregorio, M. Ahmadi and M. Buehler, *IEEE Transactions on Systems, Man, and Cybernetics, Part B* **27**, p. 626634 (1997).
13. A. De, G. Lynch, A. Johnson and D. Koditschek, Motor sizing for legged robots using dynamic task specification, in *IEEE International Conference on Technologies for Practical Robot Applications*, (Boston, MA, USA, 2011).
14. Maxon Motors, Maxon Catalog (2010–2011).
15. P. Ringegni, M. Actis and A. Patanella, *Measurement* **29**, 63 (2001).
16. T. W. Mather and M. Yim, Modular configuration design for a controlled fall, in *Intelligent Robots and Systems*, (St. Louis, USA, 2009).

---

effective inertia by mounting the tail near XRL's mass center, our analysis suggests that relocating the mount at the body's extreme end would still result in a viable design.